

# Quark confinement and the bosonic string

Martin Lüscher\*

*CERN, Theory Division  
CH-1211 Geneva 23, Switzerland*

Peter Weisz

*Max-Planck-Institut für Physik  
D-80805 Munich, Germany*

---

## Abstract

Using a new type of simulation algorithm for the standard SU(3) lattice gauge theory that yields results with unprecedented precision, we confirm the presence of a  $\gamma/r$  correction to the static quark potential at large distances  $r$ , with a coefficient  $\gamma$  as predicted by the bosonic string theory. In both three and four dimensions, the transition from perturbative to string behaviour is evident from the data and takes place at surprisingly small distances.

---

## 1. Introduction

The idea that the pure SU(3) gauge theory (and all other non-abelian gauge theories) might be closely related to some kind of string theory has been around for a long time. A comparatively direct connection derives from the observation that the gauge field generated by two widely separated static quarks appears to be squeezed into a flux tube. Such flux tubes may be expected to behave like strings with fixed ends, at least in the limit where they are very much longer than wide.

---

\* On leave from Deutsches Elektronen-Synchrotron DESY, D-22603 Hamburg, Germany

On a more formal level it has been suggested that the expectation values of large Wilson loops are matched by the corresponding amplitudes of an effective bosonic string theory [1]. Assuming this to be the case, the static quark potential  $V(r)$  can be shown to have an asymptotic expansion

$$V(r) = \sigma r + \mu + \gamma/r + O(1/r^2), \quad \gamma = -\frac{\pi}{24}(d-2), \quad (1.1)$$

at large distances  $r$ , where  $\sigma$  denotes the string tension,  $\mu$  a regularization-dependent mass and  $d$  the dimension of space-time [2,3]. The  $\gamma/r$  correction in this formula is a quantum effect that is characteristic of the relativistic bosonic string. It is universal in the sense that the value of  $\gamma$  is the same for a large class of string actions.

In principle the validity of eq. (1.1) can be checked by putting the theory on a lattice and by calculating  $V(r)$  through numerical simulation. The statistical and systematic errors in these computations are, however, rapidly increasing at large distances, and it is then practically impossible to clearly separate the  $\gamma/r$  correction from the other terms (if the standard simulation algorithms are used). As a result, we would find it difficult to claim, on the basis of the published simulation data alone, that the expansion holds with the quoted value of  $\gamma$ .

There is nevertheless some support from lattice gauge theory for the string model. It has been noted, for example, that the data for the potential at distances between 0.4 and 0.8 fm agree with eq. (1.1) within small errors [4]. Another numerical study that we wish to mention here is the work of Caselle et al. [5] on the confinement phase of the  $\mathbb{Z}_2$  gauge theory in three dimensions. Highly efficient simulation techniques are available in this case, and using these it was possible to confirm that the expectation values of large rectangular Wilson loops are matched by the string theory amplitudes to a precision where the subleading string effects can be clearly identified.

Last year we proposed a new type of simulation algorithm for the SU(3) gauge theory that leads to an exponential reduction of the statistical errors in calculations of the Polyakov loop correlation function [6]. Similar to the expectation values of Wilson loops, the latter can serve as a probe for string effects [7,8], and the onset of string behaviour may in fact be easier to observe in this way [9]. In the present paper, though, the correlation function only appears at an intermediate stage. The computations are well adapted to the new algorithm, and the results that we obtain for the force  $V'(r)$  and the second derivative  $V''(r)$  are sufficiently precise for the question raised above to be addressed.

## 2. Polyakov loop correlation function

In this section we recall some well-known facts about the Polyakov loop correlation function in the SU(3) gauge theory. The notation is the same as in ref. [6], except that we now consider the theory also in three dimensions.

### 2.1 Definition

We set up the lattice theory in the standard manner on a 4-dimensional hypercubic or 3-dimensional cubic lattice with spacing  $a$ , time-like extent  $T$  and spatial size  $L$ . Periodic boundary conditions are imposed in all directions, and for the gauge field action we take the Wilson plaquette action  $S[U]$  with bare gauge coupling  $g_0$  [10].

For any given gauge field configuration  $U(x, \mu)$ , the Polyakov loop

$$P(x) = \text{tr} \{U(x, \mu)U(x + a\hat{\mu}, \mu) \dots U(x + (T - a)\hat{\mu}, \mu)\}_{\mu=0} \quad (2.1)$$

is the trace of the Wilson line that passes through  $x$  and that winds once around the world along the time axis ( $\hat{\mu}$  denotes the unit vector in direction  $\mu$ ). We are then interested in the correlation function

$$\langle P(x)^* P(y) \rangle = \frac{1}{\mathcal{Z}} \int \mathcal{D}[U] P(x)^* P(y) e^{-S[U]}, \quad \mathcal{D}[U] = \prod_{x, \mu} dU(x, \mu), \quad (2.2)$$

where  $\mathcal{Z}$  is a normalization factor such that  $\langle 1 \rangle = 1$  and  $dU(x, \mu)$  stands for the normalized invariant measure on SU(3).

### 2.2 Spectral representation

An important property of the Polyakov loop correlation function is that it can be written as a ratio of partition functions. The transfer matrix formalism must be invoked to show this, but the derivation is then fairly straightforward (for an introduction to the subject, see refs. [11–14] for example).

First recall that the quantum mechanical states of the theory are represented by wave functions on the space of all spatial lattice gauge fields  $U$  at time  $x_0 = 0$ . The transfer matrix in the temporal gauge,  $\mathbb{T} \equiv e^{-\mathbb{H}a}$ , is a bounded hermitian operator that acts on these functions. In this framework the gauge-invariant wave functions describe the physical states in the vacuum sector, and the wave functions with two colour indices that transform according to

$$\psi_{\alpha\beta}[U^\Lambda] = \Lambda(x)_{\alpha\gamma} [\Lambda(y)_{\beta\delta}]^* \psi_{\gamma\delta}[U] \quad (2.3)$$

under gauge transformations  $\Lambda$  (where  $U^\Lambda$  denotes the gauge transform of  $U$ ) describe states with a static quark at the point  $x$  and a static antiquark at  $y$ .

If we introduce the projector  $\mathbb{P}$  to the subspace of gauge-invariant wave functions, and similarly the projector  $\mathbb{P}_{\mathbf{3} \otimes \mathbf{3}^*}(x, y)$  to the subspace of wave functions (2.3), the partition functions in these sectors are given by

$$\mathcal{Z} = \text{Tr} \{ \mathbb{P} e^{-\mathbb{H}T} \}, \quad (2.4)$$

$$\mathcal{Z}_{\mathbf{3} \otimes \mathbf{3}^*}(x, y) = \frac{1}{9} \text{Tr} \{ \mathbb{P}_{\mathbf{3} \otimes \mathbf{3}^*}(x, y) e^{-\mathbb{H}T} \}. \quad (2.5)$$

A conventional normalization factor has been included here to compensate for the trivial degeneracy of the states in the multiplets (2.3). The partition function (2.5) is thus effectively a sum over multiplets.

By inserting the explicit expression for the transfer matrix, both partition functions can be rewritten in the form of functional integrals on the  $d$ -dimensional lattice. Using an  $\text{SU}(3)$  character relation, it is then possible to establish the identity

$$\langle P(x)^* P(y) \rangle = \frac{\mathcal{Z}_{\mathbf{3} \otimes \mathbf{3}^*}(x, y)}{\mathcal{Z}}. \quad (2.6)$$

The spectrum of the transfer matrix is purely discrete in finite volume, and since the ground state in the vacuum sector is non-degenerate [12,13], an immediate consequence of this representation is that

$$\langle P(x)^* P(y) \rangle = \sum_{n=0}^{\infty} w_n e^{-E_n T} \quad (2.7)$$

for some positive energies  $E_n$  and *integral* weights  $w_n$ .

### 2.3 Relation to the potential $V(r)$

We shall only consider the potential along the lattice axes and thus set  $y = x + r\hat{\mu}$ ,  $\mu = 1$ , in the following. If we arrange the energy values in eq. (2.7) in ascending order, it is clear that  $E_0$  is the lowest energy (above the ground state energy) in the sector with the static quarks. In other words,  $E_0$  coincides with the static quark potential  $V(r)$ .

The associated eigenstate can be shown to be non-degenerate at strong coupling, and in our numerical studies of the Polyakov loop correlation function we have always found that  $w_0 = 1$ . It is usually fairly easy to obtain this result, since  $w_0$  is known

to be a positive integer. We thus conclude that

$$V(r) = -\frac{1}{T} \ln \langle P(x)^* P(y) \rangle + \varepsilon, \quad (2.8)$$

where

$$\varepsilon = \frac{1}{T} \{w_1 e^{-\Delta E T} + \dots\}, \quad \Delta E = E_1 - E_0. \quad (2.9)$$

In particular, no fits are required to extract the potential from the Polyakov loop correlation function once the latter has been computed at large values of  $T$ , where the error  $\varepsilon$  is negligible.

### 3. Bosonic string theory

The following paragraphs contain a brief description of the string theory representation of the Polyakov loop correlation function. It is included here mainly for the reader's convenience, but also to prepare the ground for the analysis of the simulation data.

#### 3.1 Effective action

In the bosonic string theory the Polyakov loop correlation function is formally given by a functional integral over all two-dimensional surfaces (world-sheets) that are bounded by the loops [1]. When both  $T$  and  $r$  are large with respect to the scale set by the string tension  $\sigma$ , the integral is dominated by the surface with the minimal area and can be calculated by expanding the integrand around this surface [2].

The important degree of freedom in this situation is the deviation of the fluctuating surface from the minimal surface in the directions orthogonal to the latter (fig. 1). If we parameterize the minimal surface through two cartesian coordinates  $z_a$  ( $a = 0, 1$ ) in the obvious way, the deviation is a vector field

$$h(z) = (0, 0, h_2(z), \dots, h_{d-1}(z)) \quad (3.1)$$

with  $d-2$  non-zero transverse components that satisfy Dirichlet boundary conditions at  $z_1 = 0$  and  $z_1 = r$ . The associated effective action may depend on how precisely

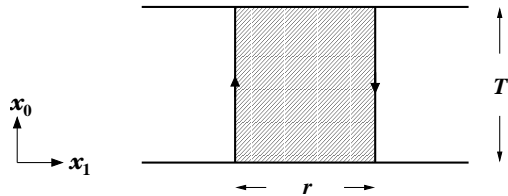


Fig. 1. In the effective string theory, the Polyakov loop correlation function is obtained by expanding the associated string partition function about the minimal surface (shaded area) spanned by the loops.

the underlying bosonic string theory was set up, but for symmetry reasons it has to be of the form

$$S_{\text{eff}} = \int_0^T \int_0^r dz_0 dz_1 \left\{ \frac{1}{2} \partial_a h \partial_a h + \dots \right\}, \quad (3.2)$$

where the ellipses stand for higher-dimensional interaction terms that are Lorentz-invariant polynomials in the derivatives of  $h$  [3]. In this context the field  $h$  is counted as dimensionless and it is, therefore, natural to assume from the beginning that the displacement of the fluctuating surface in physical units is  $h/\sqrt{\sigma}$  rather than  $h$ .

From a purely technical point of view, the effective string theory outlined above is a two-dimensional quantum field theory on the world-sheet parameter space with specified boundary conditions. Since the coefficients of the possible interaction terms are dimensionful, the perturbation expansion generated by the effective action is non-renormalizable, and counterterms of increasing dimension thus need to be included to cancel the divergent parts of the loop diagrams.

### 3.2 Leading-order approximation

If we neglect the interaction terms in the effective action (3.2), the functional integral over all vector fields  $h(z)$  can be evaluated exactly. This leads to the expression

$$\langle P(x)^* P(y) \rangle = e^{-\sigma r T - \mu T} [\det(-\Delta)]^{-\frac{1}{2}(d-2)}, \quad (3.3)$$

where  $\Delta$  denotes the laplacian on a two-dimensional cylinder of height  $r$  and circumference  $T$  with Dirichlet boundary conditions. The mass  $\mu$  that appears in this formula is a free parameter of the string model whose value has no particular physical meaning. In the gauge theory there is in fact a similar normalization ambiguity, once the need for renormalization of the Polyakov loop correlation function is taken into account [15,16].

The determinant of the laplacian can be computed explicitly using the  $\zeta$ -function finite-part prescription or one of the standard regularization methods. Such calculations have been performed in refs. [17,7,5], for example, and also in many papers on conformal field theory and fundamental string theory (see refs. [18,19] for a review and a list of references). In terms of the Dedekind  $\eta$ -function,

$$\eta(q) = q^{\frac{1}{24}} \prod_{n=1}^{\infty} (1 - q^n), \quad (3.4)$$

the result is

$$\det(-\Delta) = \eta(q)^2, \quad q = e^{-\pi T/r}, \quad (3.5)$$

from which we immediately deduce that the string amplitude on the right-hand side of eq. (3.3) admits an expansion of the form (2.7), with energies and weights

$$E_n = \sigma r + \mu + \frac{\pi}{r} \left\{ -\frac{1}{24}(d-2) + n \right\}, \quad (3.6)$$

$$w_0 = 1, \quad w_1 = d-2, \quad w_2 = \frac{1}{2}(d-2)(d+1), \quad \text{etc.} \quad (3.7)$$

In particular, to this order of the effective string theory, the static quark potential is given by eq. (1.1) (without any corrections proportional to higher powers of  $1/r$ ) and the energy gap  $\Delta E$  is equal to  $\pi/r$ .

### 3.3 Higher orders $\mathcal{E}$ renormalization

Quantum field theories on space-time manifolds with boundaries require, in general, the inclusion of terms in the action that are localized at the boundary [20,21]. In the present case the simplest term of this type is

$$S_1 = \frac{1}{4}b \int_0^T dz_0 \left\{ (\partial_1 h \partial_1 h)_{z_1=0} + (\partial_1 h \partial_1 h)_{z_1=r} \right\}, \quad (3.8)$$

where  $b$  is a parameter of dimension [length]. The effect of  $S_1$  on the Polyakov loop correlation function can be easily worked out to first order in  $b$  using the  $\zeta$ -function finite-part prescription, for example. For the static potential and the energy gap the calculation yields

$$V(r) = \sigma r + \mu - \frac{\pi}{24r} (d-2) (1 + b/r), \quad (3.9)$$

$$\Delta E = \frac{\pi}{r} (1 + b/r). \quad (3.10)$$

As expected these corrections are negligible compared to the leading-order terms at sufficiently large values of  $r$ .

It can be shown that the boundary action  $S_1$  is the only term with a coefficient of dimension 1 that can occur in the effective action. There are just a few more terms with coefficients of dimension [length]<sup>2</sup>, such as

$$S_2 = \frac{1}{4}c_2 \int_0^T \int_0^r dz_0 dz_1 (\partial_a h \partial_a h) (\partial_b h \partial_b h). \quad (3.11)$$

They give rise to corrections to the static quark potential proportional to  $1/r^3$ , i.e. to terms that are even more suppressed at large distances.

A more careful discussion of the higher-order contributions must take into account the fact that the theory needs to be regularized. This introduces another scale, the ultra-violet cutoff  $\Lambda$ , and corrections proportional to  $(c_2/r^3)(\Lambda r)^p$ , for example, must then be expected to arise. However, as in any other non-renormalizable field theory, it must be possible to cancel the divergent contributions by a renormalization of  $\sigma$ ,  $\mu$  and the coefficients of the interaction terms.

For illustration we note that a term proportional to  $c_2\Lambda/r^2$  actually does occur if a lattice regularization is used. In this case the inclusion of the boundary term  $S_1$  is thus required to be able to renormalize the theory. The bottom line is then that equations like (3.9) and (3.10) hold to all orders of the renormalized effective theory, up to corrections proportional to higher powers of  $1/r$ .

#### 4. Numerical evaluation of $V(r)$ and its derivatives

Using the simulation algorithm of ref. [6], the Polyakov loop correlation function can be computed at values of  $T$  and  $r$  that previously appeared to be inaccessible. In particular, when  $T$  is increased at fixed  $r$ , the computer time required for a specified *relative* statistical error is only growing approximately like  $T^3$ , while the signal is exponentially decreasing. This enables us to obtain the static quark potential  $V(r)$  via eq. (2.8) with small errors.

The effective string theory predicts that the force  $F(r) = V'(r)$  decreases towards the string tension  $\sigma$  at large distances  $r$  with a rate proportional to  $1/r^2$ . In this



paper our principal goal is to find out whether the numerical data are consistent with this and whether the slope

$$c(r) = \frac{1}{2}r^3 F'(r) \tag{4.1}$$

converges to the value of the universal coefficient  $\gamma$  in eq. (1.1). We are, therefore, more interested in the derivatives of the static potential than in the potential itself.

#### 4.1 Lattice definition of $F(r)$ and $c(r)$

There is no unique way to “differentiate” lattice functions, but a sensible prescription should evidently be such that the correct continuum limit is obtained and that no artificially large lattice effects are introduced. The definition of  $F(r)$  proposed by Sommer [22] fulfils this condition and is easily extended to  $c(r)$ . We are thus led to define

$$F(\bar{r}) = \{V(r) - V(r - a)\}/a, \tag{4.2}$$

$$c(\tilde{r}) = \frac{1}{2}\tilde{r}^3 \{V(r + a) + V(r - a) - 2V(r)\}/a^2, \tag{4.3}$$

where  $\bar{r}(r)$  and  $\tilde{r}(r)$  satisfy

$$\bar{r} = r - \frac{1}{2}a + O(a^2), \tag{4.4}$$

$$\tilde{r} = r + O(a^2). \tag{4.5}$$

The precise choice of these functions takes into account the approximate shape of the potential, so that an enhancement of lattice effects is avoided, particularly at small distances [22,4]. Explicitly we set

$$\bar{r}^{2-d} = 2\pi(d - 2)\{G(r - a) - G(r)\}/a, \tag{4.6}$$

$$\tilde{r}^{1-d} = 2\pi\{G(r + a) + G(r - a) - 2G(r)\}/a^2, \tag{4.7}$$

where  $G(r)$  denotes the value of the Green function of the lattice laplacian in  $d - 1$  dimensions at the point  $(r, 0, \dots, 0)$  (for a detailed discussion of the Green function in two and three dimensions, see refs. [23,4] for example).

#### 4.2 Systematic errors

Lattice spacing effects, the omission of the contribution of the higher-energy states in eq. (2.8) and finite-volume effects are sources of systematic uncertainties in our calculations. As usual the lattice effects can be controlled by performing simulations at several values of the lattice spacing, and we shall return to this issue in sect. 5 when we discuss the simulation results.

To estimate the error  $\varepsilon$  in eq. (2.8), some information on the energy values  $E_n$  and the associated weights  $w_n$  is needed. Accurate data for the lowest excited levels were first obtained by Michael and Perantonis [24], and more precise and extensive studies have later been reported by Juge, Kuti and Morningstar [25,26]. The results show that, in four dimensions, the gap  $\Delta E$  is about  $2.2/r$  at the Sommer reference scale  $r = r_0$ . It then approaches  $\pi/r$  around  $r = 3r_0$  and stays above this value at still larger distances. The associated weight  $w_1$  is 2 as in the effective string theory. Using this and the fact that the higher levels are well separated from  $E_1$ , the error in eq. (2.8) can be estimated straightforwardly.

There are unfortunately no results on the spectrum of the excited levels in three dimensions, and we can only refer to the analogous case of the SU(2) theory, where the situation does not appear to be very different from the one described above [26]. We have, therefore, estimated the error in eq. (2.8) in the same way, with  $w_1 = 1$ , and checked the estimate by performing simulations at various values of  $T$ .

Finite-volume effects can arise when the colour flux tube is squeezed in the transverse directions by the finite extent of the lattice. In all our calculations the spatial lattice size  $L$  was at least 20 times larger than the bulk correlation length [27,28], and these effects were thus suppressed by many orders of magnitude. Another systematic effect can be traced back to the presence of states where the flux tube is winding “around the world”. The energy of these states is at least  $V(L - r)$ , and their contribution to the error in eq. (2.8) will therefore be small if  $L$  and  $r$  are such that  $V(L - r) - V(r)$  is large.

#### 4.3 Statistical errors

The parameters of the simulation algorithm of ref. [6] can be chosen so that subsequent “measurements” of the Polyakov loop correlation function may be assumed to be statistically independent. We have done so and later confirmed the independence of the data by determining the integrated autocorrelation time. The standard single-elimination jackknife analysis was then applied to calculate the statistical errors.

An important property of the data series generated in this way is that the values of the static potential at different distances turn out to be very strongly correlated.

Table 1. Simulation parameters

$d$	$\beta$	$r_0/a$	$a$ [fm]	$r_{\max}/a$	$T/a$	$L/a$
4	5.70	2.93	0.171	7	24	18
4	5.85	4.09	0.122	9	36	24
4	6.00	5.39	0.093	12	48	30
3	11.0	3.30	0.152	9	32	24
3	15.0	4.83	0.104	12	48	32
3	20.0	6.71	0.075	14	60	36

As a consequence there is a significant cancellation of statistical errors when the force  $F(r)$  and the slope  $c(r)$  are calculated. It is then also profitable to keep track of the statistical correlations in the further analysis of the data.

## 5. Simulation results

In table 1 we list the values of the coupling  $\beta = 6a^{d-4}/g_0^2$  and other important parameters of the simulations that we have performed. The entries in the last three columns are the maximal distance and the associated lattice sizes where we have accurate results for the Polyakov loop correlation function. At smaller distances, the lattices do not need to be as large, but were always chosen so that the systematic errors (other than the lattice effects) are sufficiently suppressed. Further algorithmic details and a collection of data tables are included in appendices A and B.

In the following we first discuss the results at the smallest values of the lattice spacing and shall then argue (in subsect. 5.3) that the lattice effects at these points are already very small.

### 5.1 $F(r)$ and $c(r)$ in four dimensions

One of the striking results of our computations is that the force  $F(r)$  appears to be a linear function of  $1/r^2$  in the range  $r \geq 0.5$  fm (see fig. 2). The errors on the data points shown in this figure increase from below 0.04% to about 0.12% at the left-most point, and the four points at the largest values of  $r$  lie on a straight line to this level of accuracy.

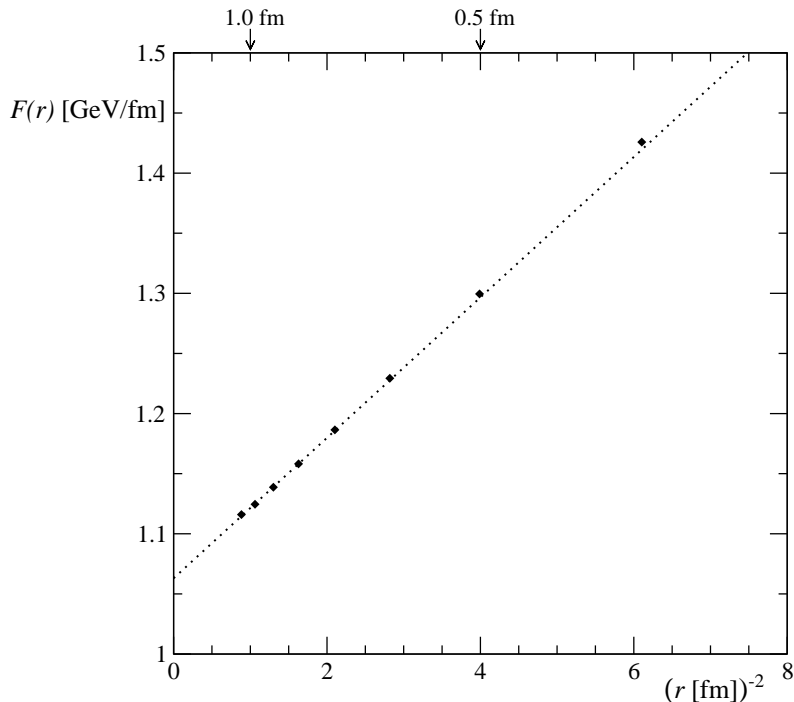


Fig. 2. Force  $F(r)$  in the four-dimensional theory versus  $1/r^2$  at  $\beta = 6.0$ . Physical units are set by the Sommer scale  $r_0 = 0.5$  fm [22] and the dotted line is a linear fit to the four points at the largest distances. Errors are smaller than the data symbols.

There is still some curvature in the data, which is more clearly seen in fig. 3 where we plot the slope  $c(r)$ . The errors on these points are at most 2.5% and significantly less than this at the smaller distances. Note that  $c(r)$  can be interpreted as a running coupling,

$$c(r) = -\frac{4}{3}\alpha(1/r), \quad \alpha(\mu) = \frac{\bar{g}(\mu)^2}{4\pi}, \quad (5.1)$$

that satisfies the usual perturbative renormalization group equation

$$\mu \frac{\partial \bar{g}}{\partial \mu} = - \sum_{n=0}^{\infty} b_n \bar{g}^{2n+3}. \quad (5.2)$$

The coefficients  $b_n$  are known up to three-loop order in this scheme [29–33], and using these we can integrate eq. (5.2) from  $r = 0$ , taking the  $\Lambda$  parameter determined in refs. [34,35] as the initial condition.

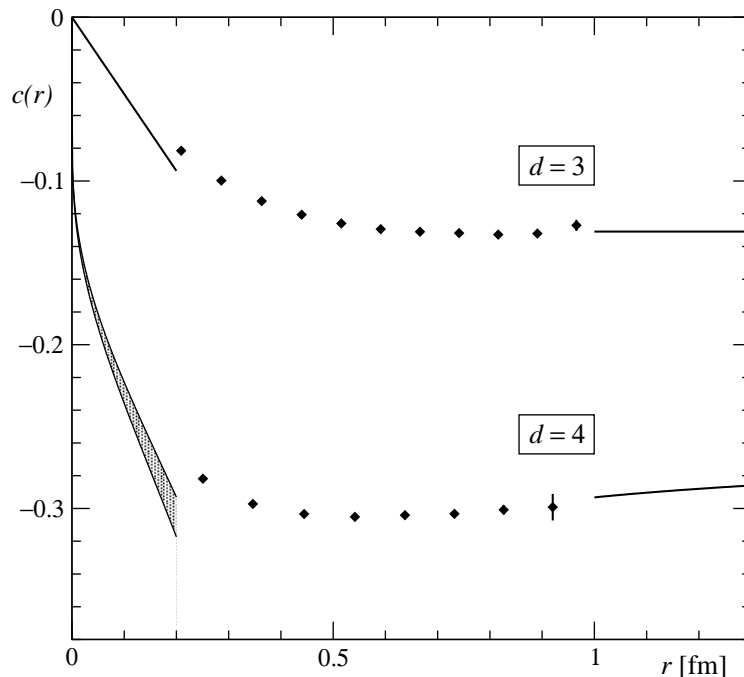


Fig. 3. Slope  $c(r)$  in three and four dimensions at  $\beta = 20.0$  and  $\beta = 6.0$  respectively. The curves on the left are obtained from perturbation theory, while those on the right derive from the string theory formula (3.9) with  $b = 0$  and  $b = 0.04$  fm.

In the related case of the force  $F(r)$ , the range of applicability of the perturbation expansion extends to distances of around 0.2 or at most 0.3 fm [36]. We refer to this paper for further details and only remark that the error on the  $\Lambda$  parameter alone results in a significant spread of the three-loop curves shown in fig. 3 (shaded area on the left). It is in any case evident from the plot that  $c(r)$  breaks away from the perturbative behaviour near  $r = 0.2$  fm.

At larger distances the data show a shallow minimum and then gently increase to about  $-0.293$  at  $r = 1$  fm. This is still 12% away from  $\gamma = -0.262$ , but not really inconsistent with the effective string theory, because the correction proportional to  $b$  in eq. (3.9) (and possibly higher-order terms) may not be negligible at these distances. As shown in fig. 3 we can in fact easily make contact with the data if we allow for such a correction.

### 5.2 Three-dimensional theory

In three dimensions the static potential at short distances has a completely different shape, but the effective string theory predicts the same behaviour at large distances, with a coefficient  $\gamma$  that is precisely half as big as in four dimensions.

Our numerical results fully agree with this (see fig. 3). No  $b/r$  correction is required in this case to match the data points at the largest distances, while at the smaller values of  $r$  we observe a smooth transition from perturbative to string behaviour. In this theory the perturbation expansion to two-loop order reads [32]

$$c(r) = -\frac{1}{3\pi}g^2r + \mathcal{O}(g^6), \quad (5.3)$$

where  $g$  denotes the gauge coupling in the continuum limit. To express the coupling in physical units, we used the conversion factor  $g^2r_0 = 2.2$  (which can be inferred from our data) and set  $r_0 = 0.5$  fm as usual.

### 5.3 Lattice effects

In both three and four dimensions, we have simulated lattices at different values of the lattice spacing in order to study the approach of the force  $F(r)$  and the slope  $c(r)$  to the continuum limit (see table 1). The comparison of the data produced in these simulations requires all dimensionful quantities to be scaled to some physical units. It is natural to take the Sommer radius  $r_0$  as the basic reference scale in the present context, and we shall thus be interested in determining the lattice-spacing dependence of the dimensionless functions  $r_0^2F(xr_0)$  and  $c(xr_0)$  in a range of the scale factor  $x$ .

Since the distances  $xr_0$  are in general fractional multiples of the lattice spacing, an interpolation formula must be specified. Given the approximate shape of  $F(r)$  and  $c(r)$ , we decided to use a three-point polynomial interpolation in  $1/x^2$  and  $1/x$  respectively. Note that it would be logically incorrect to assign a systematic error to the interpolation, because the latter merely defines the functions between the lattice points. On the other hand, a poor choice of the interpolation formula will lead to artificially enhanced lattice effects.

From the tables in appendix B it is clear that the lattice effects are quite small at the lattice spacings considered. In both three and four dimensions, the residual effects on the lattices with the smallest spacing are probably no more than about 0.1% in the case of the force  $r_0^2F(xr_0)$  and 1–2% in the case of the slope  $c(xr_0)$ . The theoretically expected scaling proportional to  $a^2$  [37,4] is, however, not observed, at least not in four dimensions, where the lattice effects at  $\beta = 5.7$  appear to be larger than what would be inferred from the other lattices.

For this reason, and since we have data at only three values of the lattice spacing, we do not attempt to perform an extrapolation to the continuum limit. We would in any case not expect the extrapolation to have any impact on the outcome of our work, because the lattice effects are small and because in four dimensions the values of  $c(xr_0)$  at the larger distances  $xr_0$  would only be moved closer to  $\gamma$ .

## 6. Conclusions

The results reported in this paper show that string behaviour in the static potential sets in at quark-antiquark separations around 0.5 fm. In three dimensions the confirmation of the string theory formula (1.1) is particularly impressive, while in four dimensions a small higher-order correction needs to be included to match the data points at the largest distances in fig. 3.

The observed agreement with the effective string theory is somewhat surprising and in fact difficult to understand, because the physical picture of a thin fluctuating flux tube is hardly correct at these distances. Perhaps this is an indication of the existence of an exact dual formulation of  $SU(N)$  gauge theories in terms of a fundamental string theory, along the lines of ref. [38] for example, from which the effective theory derives. Note that not only the general form of the effective action, but also the values of the coefficients of the higher-dimensional terms would be predictable in this case (to the extent the fundamental string theory is tractable).

Another logical possibility is that eq. (1.1) may have a different origin and that the proper interpretation of our results still needs to be found. It has been pointed out in this connection that the spectrum of the excited levels  $E_n$  does not appear to agree with the one obtained at leading order of the effective string theory [25,26]. Whether this rules out the effective theory is not completely obvious, however, because the observed discrepancies (which are significant even at distances  $r \geq 2$  fm) could be a result of the higher-order corrections. In particular, the accidental degeneracies of the spectrum at leading order probably disappear once the non-linear interactions are switched on.

A systematic study of the higher-order effects would now be required to resolve this issue. Accurate calculations of the lowest energy values in each symmetry sector may then already provide enough information to determine the coefficients of the few leading terms in the effective action. It would evidently also be interesting to see whether our results carry over to other non-abelian gauge groups and to all representations of the Wilson lines with non-trivial transformation behaviour under

the centre of the gauge group. We finally note that the computation of  $c(r)$  at distances larger than reported here rapidly requires enormous amounts of computer time, because the significance loss in eq. (4.3) (which grows proportionally to  $\sigma r^4/a^2$ ) must be compensated by increasing the statistics.

*Acknowledgements:* We are indebted to Christina Diamantini, Julius Kuti, Rainer Sommer, Poul Olesen and Yaron Oz for helpful correspondence and discussions, and to Julius in particular for sending us a draft of his forthcoming long paper with Jimmy Juge and Colin Morningstar on the spectrum of the energy values  $E_n$ . Our computations have been performed on PC-clusters at DESY (Hamburg and Zeuthen), at the Max-Planck-Institut für Physik in Munich and at the Fermi Institute in Rome. We wish to thank the directors of these institutions for having made this possible, and Peter Breitenlohner, Filippo Palombi, Peter Wegner and Hartmut Wittig for technical support.

## Appendix A. Simulation algorithm

The multilevel algorithm that was used in the present study is described in detail in ref. [6]. Here we merely wish to add a few comments on performance and optimization issues.

All tests of the algorithm reported in ref. [6] were carried out on four-dimensional lattices at  $\beta = 5.7$ . We now confirm that it performs well also at larger values of  $\beta$  and in three dimensions. For illustration we quote the computation of the Polyakov loop correlation function at  $\beta = 6.0$ ,  $T = 48a$  and  $r = 12a$ . This is an extreme case where the area of the minimal surface bounded by the loops reaches  $5 \text{ fm}^2$ . The correlation function is very small at this point (about  $1.1 \times 10^{-25}$ ), but with one month of running time on a PC-cluster with 24 Pentium 4 processors it was possible to determine its value to an accuracy better than 3%.

Contrary to what may be understood from ref. [6], the more complicated forms of the algorithm, with many levels of nested averages, are often not worth while. Most of our results have in fact been obtained with only one level, but a relatively large number (up to a few thousands) of “measurements” of the two-link operators on the associated time slices. An important side effect of such high numbers of time-slice updates is that the statistical correlations between the data at the distances covered in a given run tend to be enhanced (cf. subsect. 4.3).

For future applications of the multilevel algorithm at larger distances  $r$ , it may be



necessary to study and improve its efficiency at the level of the time-slice averages. There is currently no understanding of the autocorrelation times in this subsystem, and rather than increasing the statistics, there may be better ways to cope with the exponential decay of the averaged two-link operators.

## Appendix B. Data tables

In tables 2–7 we only list the most important results for the force  $F(r)$  and the slope  $c(r)$ . More detailed data tables, including error correlation matrices, may be obtained from the authors in electronic form.

Table 2. Simulation results at  $\beta = 6.0$  in 4 dimensions

$r/a$	$\bar{r}/a$	$a^2 F(\bar{r})$	$\tilde{r}/a$	$c(\tilde{r})$
3	2.277	0.102491(20)	2.700	0.28184(10)
4	3.312	0.073854(22)	3.729	0.29724(18)
5	4.359	0.062399(24)	4.786	0.30339(38)
6	5.393	0.056871(25)	5.833	0.30515(70)
7	6.414	0.053800(27)	6.864	0.3041(12)
8	7.428	0.051924(30)	7.886	0.3033(17)
9	8.438	0.050687(34)	8.901	0.3008(28)
10	9.445	0.049834(38)	9.912	0.2992(80)
11	10.451	0.049213(46)		
12	11.455	0.048839(72)		

Table 3. Simulation results at  $\beta = 20.0$  in 3 dimensions

$r/a$	$\bar{r}/a$	$a^2 F(\bar{r})$	$\tilde{r}/a$	$c(\tilde{r})$
3	2.379	0.0508627(32)	2.808	0.081536(41)
4	3.407	0.0434942(32)	3.838	0.099772(77)
5	4.432	0.0399646(33)	4.875	0.112270(96)
6	5.448	0.0380274(35)	5.902	0.12057(13)
7	6.458	0.0368546(38)	6.920	0.12596(23)
8	7.464	0.0360941(41)	7.932	0.12945(41)
9	8.469	0.0355749(45)	8.941	0.13100(55)
10	9.473	0.0352080(49)	9.948	0.13184(69)
11	10.475	0.0349401(55)	10.953	0.13276(92)
12	11.478	0.0347382(62)	11.957	0.1321(17)
13	12.480	0.0345838(73)	12.961	0.1271(34)
14	13.481	0.0344673(92)		

Table 4. Values of  $r_0^2 F(xr_0)$  in 4 dimensions

$x$	$\beta = 5.70$	$\beta = 5.85$	$\beta = 6.00$
0.8	1.82181(23)	1.82203(57)	1.82041(16)
1.0	1.65	1.65	1.65
1.2	1.55341(12)	1.55602(34)	1.55691(18)
1.4	1.49372(23)	1.49983(49)	1.50100(36)
1.6	1.45561(31)	1.46369(60)	1.46476(51)
1.8	1.42963(39)	1.43920(76)	1.44010(70)
2.0	1.41122(47)	1.4217(10)	1.4230(11)

Table 5. Values of  $r_0^2 F(xr_0)$  in 3 dimensions

$x$	$\beta = 11.0$	$\beta = 15.0$	$\beta = 20.0$
0.8	1.720701(26)	1.719410(57)	1.718083(52)
1.0	1.65	1.65	1.65
1.2	1.608316(37)	1.610380(53)	1.610988(73)
1.4	1.582508(55)	1.58583(10)	1.58689(12)
1.6	1.565497(77)	1.56965(14)	1.57112(16)
1.8	1.553860(90)	1.55852(19)	1.56022(22)
2.0	1.54555(11)	1.55048(24)	1.55271(34)

Table 6. Values of  $c(xr_0)$  in 4 dimensions

$x$	$\beta = 5.70$	$\beta = 5.85$	$\beta = 6.00$
1.0	-0.31427(43)	-0.3067(10)	-0.30493(58)
1.2	-0.32150(57)	-0.3048(14)	-0.3045(11)
1.4	-0.32113(72)	-0.3036(13)	-0.3039(15)
1.6	-0.3176(10)	-0.3003(22)	-0.3014(24)
1.8	-0.3150(19)	-0.2990(50)	-0.2995(64)

Table 7. Values of  $c(xr_0)$  in 3 dimensions

$x$	$\beta = 11.0$	$\beta = 15.0$	$\beta = 20.0$
1.0	-0.13225(14)	-0.12696(18)	-0.12505(21)
1.2	-0.13842(16)	-0.13157(32)	-0.12972(40)
1.4	-0.14106(30)	-0.13475(40)	-0.13144(55)
1.6	-0.14153(33)	-0.13552(67)	-0.13273(84)
1.8	-0.14106(52)	-0.13654(97)	-0.1316(18)

## References

- [1] Y. Nambu, Phys. Lett. B80 (1979) 372
- [2] M. Lüscher, K. Symanzik, P. Weisz, Nucl. Phys. B173 (1980) 365
- [3] M. Lüscher, Nucl. Phys. B180 (1981) 317
- [4] S. Necco, R. Sommer, Nucl. Phys. B622 (2002) 328
- [5] M. Caselle, R. Fiore, F. Gliozzi, M. Hasenbusch, P. Provero, Nucl. Phys. B486 (1997) 245
- [6] M. Lüscher, P. Weisz, J. High Energy Phys. 09 (2001) 010
- [7] J. Ambjørn, P. Olesen, C. Peterson, Phys. Lett. B142 (1984) 410; Nucl. Phys. B244 (1984) 262
- [8] P. de Forcrand, G. Schierholz, H. Schneider, M. Teper, Phys. Lett. B160 (1985) 137
- [9] B. Lucini, M. Teper, Phys. Rev. D64 (2001) 105019
- [10] K. G. Wilson, Phys. Rev. D10 (1974) 2445
- [11] M. Lüscher, Commun. Math. Phys. 54 (1977) 283
- [12] K. Osterwalder, E. Seiler, Ann. Phys. (NY) 110 (1978) 440
- [13] E. Seiler, Gauge theories as a problem of constructive quantum field theory and statistical mechanics, Lecture Notes in Physics 159 (Springer, Berlin, 1982)
- [14] M. Lüscher, Selected topics in lattice field theory, Lectures given at Les Houches (1988), in: Fields, strings and critical phenomena, eds. E. Brézin, J. Zinn-Justin (North-Holland, Amsterdam, 1989)
- [15] V. S. Dotsenko, S. N. Vergeles, Nucl. Phys. B169 (1980) 527
- [16] R. A. Brandt, F. Neri, M. Sato, Phys. Rev. D24 (1981) 879
- [17] K. Dietz, T. Filk, Phys. Rev. D27 (1983) 2944
- [18] J. L. Cardy, Conformal invariance and statistical mechanics, Lectures given at Les Houches (1988), in: Fields, strings and critical phenomena, eds. E. Brézin, J. Zinn-Justin (North-Holland, Amsterdam, 1989)
- [19] P. Ginsparg, Applied conformal field theory, Lectures given at Les Houches (1988), in: Fields, strings and critical phenomena, eds. E. Brézin, J. Zinn-Justin (North-Holland, Amsterdam, 1989)
- [20] K. Symanzik, Nucl. Phys. B190 [FS3] (1981) 1
- [21] M. Lüscher, Nucl. Phys. B254 (1985) 52
- [22] R. Sommer, Nucl. Phys. B411 (1994) 839
- [23] D.-S. Shin, Nucl. Phys. B525 (1998) 457
- [24] S. Perantonis, C. Michael, Nucl. Phys. B347 (1990) 854
- [25] K. J. Juge, J. Kuti, C. J. Morningstar, Nucl. Phys. B (Proc.Suppl.) 63 (1998) 326; *ibid.* 73 (1999) 590; *ibid.* 83 (2000) 503; *ibid.* 106 (2002) 691

- [26] K. J. Juge, J. Kuti, C. J. Morningstar, From surface roughening to QCD string theory, in: Non-perturbative QFT methods and their applications (Budapest 2000), eds. Z. Horváth, E. Palla (World Scientific, Singapore, 2001)
- [27] C. Michael, Glueballs, hybrid and exotic mesons, and string breaking, in: Quark confinement and the hadron spectrum IV (Vienna 2000), eds. W. Lucha, K. M. Maung (World Scientific, Singapore, 2002)
- [28] M. Teper, Phys. Rev. D59 (1999) 014512
- [29] W. Fischler, Nucl. Phys. B129 (1977) 157
- [30] A. Billoire, Phys. Lett. B92 (1980) 343
- [31] M. Peter, Nucl. Phys. B501 (1997) 471
- [32] Y. Schröder, Phys. Lett. B447 (1999) 321; DESY-THESIS-1999-021
- [33] M. Melles, Phys. Rev. D62 (2000) 074019
- [34] M. Lüscher, R. Sommer, P. Weisz, U. Wolff, Nucl. Phys. B413 (1994) 481
- [35] S. Capitani, M. Lüscher, R. Sommer, H. Wittig, Nucl. Phys. B544 (1999) 669
- [36] S. Necco, R. Sommer, Phys. Lett. B523 (2001) 135
- [37] K. Symanzik, Nucl. Phys. B226 (1983) 187, 205
- [38] A. M. Polyakov, Int. J. Mod. Phys. A14 (1999) 645